Science of the Total Environment 776 (2021) 146023

Contents lists available at ScienceDirect

Science of the Total Environment

journal homepage: www.elsevier.com/locate/scitotenv

Spatial evolution of population change in Northeast China during 1992–2018

Haolin You [a,b], Jun Yang [a,b,**], Bing Xue [c,*], Xiangming Xiao [d], Jianhong Xia (Cecilia) [e], Cui Jin [b], Xueming Li [b]

[a] Jangho Architecture College, Northeastern University, Shenyang 110169, China
[b] Human Settlements Research Center, Liaoning Normal University, 116029 Dalian, China
[c] Institute of Applied Ecology, Chinese Academy of Sciences, Shenyang, Liaoning 110016, China
[d] Department of Microbiology and Plant Biology, Center for Spatial Analysis, University of Oklahoma, Norman, OK 73019, USA
[e] School of Earth and Planetary Sciences (EPS), Curtin University, Perth 65630, Australia

HIGHLIGHTS

- Understanding population mobility trends is key to urban sustainable development.
- Population loss in Northeast China has weakened the regional economy.
- We spatially analyzed night light and other data to quantify population trends.
- Population loss negatively affects population structure (e.g., increased age).
- Population loss also inconveniences government management and planning.

GRAPHICAL ABSTRACT

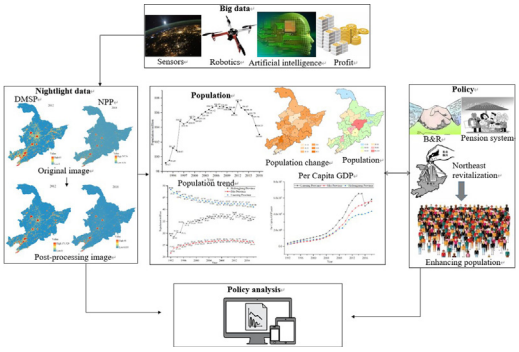

ARTICLE INFO

Article history:
Received 8 January 2021
Received in revised form 7 February 2021
Accepted 16 February 2021
Available online 22 February 2021

Editor: Philip K. Hopke

Keywords:
Population loss
Nighttime light
Image correction
Spatial change
Northeast China

ABSTRACT

In the context of rapid socioeconomic development, population mobility has become an increasingly prominent phenomenon and is profoundly influencing urban development. Therefore, when proposing strategies to rejuvenate Northeast China and promoting sustainable development in the region, it is important to explore long-term population trends and to formulate development strategies and policies accordingly. Using remote-sensing nighttime light data obtained by DMSP/OLS during 1992–2012 and NPP-VIIRS during 2012–2018 in combination with population statistics for China's three northeastern provinces, this study estimated the population of 36 prefecture-level cities and quantitatively studied population loss trends. The results showed that: (1) the three northeastern provinces have great population mobility, presenting a multi-center "T"-shaped spatial pattern with provincial capitals being the main center and population gradually decreasing toward peripheral areas, with Liaoning > Heilongjiang > Jilin in terms of overall population; (2) from 1992 to 1996, the population of the three northeastern provinces showed a positive linear growth trend, with the population increasing by 5.64×10^4 people and an average population growth rate of 2.29% over the four-year period; from 1996 to 2006, population growth slowed, with an increase of only 2.08×10^4 people over 10 years, and the average growth rate dropped to 0.18%; in 2006–2011, population growth showed a negative trend, with a population loss of 0.98×10^4 people and a decline rate of 0.31%; beginning in 2012, population loss was very serious, presenting a sharp linear decline, and by 2018, the population loss was as high as 4.46×10^6 people. Our findings indicate that population loss will result in a series of negative effects in the region, not only affecting the population growth structure but also changing the regional population structure, and inconveniencing government management and planning.

* Correspondence to: J. Yang, Jangho Architecture College, Northeastern University, Shenyang 110169, China.
** Corresponding author.
E-mail addresses: yangjun8@mail.neu.edu.cn (J. Yang), xuebing@iae.ac.cn (B. Xue), xiangming.xiao@ou.edu (X. Xiao), c.xia@curtin.edu.au (J. Xia), cuijin@lnnu.edu.cn (C. Jin).

https://doi.org/10.1016/j.scitotenv.2021.146023
0048-9697/

1. Introduction

Given China's rapidly developing society and accelerating globalization, population mobility has continuously increased. In this context, however, population loss has occurred in certain regions, which can lead to negative effects, such as intensification of population aging and imbalanced regional economic development (Nijman and Wei, 2020; Liu et al., 2020; Yang et al., 2011). According to the 2018 Report on China's Migrant Population Development released by the National Health Commission, China's migrant population was 240 million in 2017, signaling a transition from a growth period to one of adjustment (Hou and Li, 2017; Yang et al., 2020a). In 2016, to address the problems of population migration, China formally joined the International Organization for Migration. Meanwhile, the United Nations Sustainable Development Goals for 2030 recognized for the first time the contribution of migration to sustainable development and proposed that migration and population movements should happen in an orderly, safe, and responsible manner (Oke, 1973; Ferracioli, 2018). Further, existing studies suggest that appropriate population migration is crucial for adjusting population distributions and sharing economic development across regions (Chan et al., 2019; Fu et al., 2016). Therefore, as coordinated economic development is the common goal of mankind (Stewart and Oke, 2012; Adams and Page, 2005; Qiao et al., 2020), innovative millennium development goals could include making full use of natural resources and regional advantages to mitigate and cope with population loss (Fukuda-Parr and Sakiko, 2016; Guo et al., 2020; Yang et al., 2020b).

International scholars began investigating population migration earlier than researchers in China, and they mainly concentrated on policy directions, along with the causes, determinants, and spatial characteristics of population loss and its relationship with urbanization (Fan, 2005; Mitsuru, 2018; Otterstrom, 2001). Presently, studies in China have focused on the spatial distribution and attributes of population migration, its determinants, the relationship between population migration and urbanization, the influence of population migration on regional economic development, and the prediction of population migration (Yue et al., 2019; Liu and Feng, 2014; Mei et al., 2014; Sun et al., 2012; Yang et al., 2013; Yu et al., 2017). For instance, Liu et al. examined data from the 1% national sample census in 2005 and the 10% population census in 2000 to analyze the flow field of population migration across provinces and its spatial characteristics. They identified a gradually expanding scale of provincial migration, which tended to stem from regions such as Sichuan, Hunan, Jiangxi, Henan, and Anhui to southeastern coastal and economically advanced areas including the Yangtze River Delta, Pearl River Delta, and the Beijing-Tianjin-Hebei region; further, they found that the intensity of migration was increasing (Liu et al., 2012b). By comparing the 2000 and 2010 population censuses, Wang et al. identified local changes in the regional patterns of inter-provincial migration in China since the 1990s (Wang et al., 2012). Such studies on population migration mostly relied on statistics; however, given the high level of mobility and uncertainty regarding population counts, statistics can be one-sided and incomplete and yield relatively large errors in research results.

Since the Reform and Opening up, population migration has become more active in China. Domestic and international scholars, as well as the Chinese government, have devoted considerable attention to population loss in Northeast China (Lutz et al., 2003; Simini et al., 2012; Zhu et al., 2020). As Northeast China serves as an important base for heavy industries and is China's largest grain-producing region, its development has profound significance to China (He et al., 2019; Sun et al., 2012; Wang et al., 2011). However, population loss in this region has become increasingly severe and has weakened the regional economy and social development. Thus, appropriate population migration must be promoted to adjust the population distribution and balance development across regions. Leveraging natural resources and regional advantages to mitigate and cope with population loss would be an innovative method to achieve millennium development goals (He, 2018; Fukuda-Parr and Sakiko, 2016; Nash et al., 2020). In our study, we combined nighttime light (NTL) and other data with spatial analysis to quantitatively gauge the characteristics of the spatial differentiation of population and the effects of population loss in Northeast China from 1992 to 2018. Our findings will offer empirical information to support the revitalization and development of the region.

2. Materials and methods

2.1. Study area and data

2.1.1. Study area

Northeast China (also called the Three Northeast Provinces or the Three East Provinces; 120°E–135°E, 38°N–56°N), refers to Liaoning, Jilin, and Heilongjiang Provinces. These provinces have a total area of around 787,300 km^2, accounting for 8.2% of China's total land area. Specifically, there are 14 cities in Liaoning, eight cities and the Yanbian Korean Autonomous Prefecture in Jilin, and 12 cities and the Daxing'anling Prefecture in Heilongjiang (Fig. 1).

2.1.2. Data source

The data in our study included DMSP/OLS data, NPP-VIIRS data, and data from administrative divisions and population censuses, which are described in Table 1.

2.2. Research methods

2.2.1. DMSP image preprocessing

Image reprojection, resampling, and cropping. DMSP images were downloaded based on administrative boundaries in Northeast China, cropped, and then reprojected onto Lambert Conformal Conic projections with a 1-km resample resolution. Finally, we obtained the DMSP/OLS non-radiation calibrated annual NTL intensity within the administrative areas of Northeast China from 1992 to 2012 with a spatial resolution of 1 km (Cao et al., 2015).

Image intercalibration and saturation correction. The DMSP/OLS image set was acquired by the 6th Satellite Operations Group, in which two satellites collected the same data over a given year. Thus, two independent datasets exist for each year. As no on-board calibration exists for the OLS sensors, long time-series data from multiple satellites are not comparable. Moreover, the digital number (DN) values of the DMSP images were between 0 and 63, which indicates the existence of light saturation; this suggests that many saturated pixels presented a DN, and thus light intensity, that was lower than the actual value. Therefore, to improve the comparability of the data, it was necessary to perform intercalibration and saturation correction (Cao et al., 2015; Zhang et al., 2017; Zhao et al., 2019).

According to previous research, we adopted the domain-invariant approach to calibrate the images using the power function correction model with the highest correlation coefficients (Eq. (1)) (You et al., 2020).

$$DN_{cal} = a \times DN^{b} \quad (1)$$

Here, DN_{cal} refers to the DN value of the corrected pixel, while DN is the DN value of the pixel to be corrected. Further, a and b are different parameters from the power regression (Table 2) (Cao et al., 2015).

Continuity correction. After the above calibration and saturation correction, the range of the DN values of the NTL images increased from 0 to 63 to 0–171. Despite some improvements in the image quality and local details, a lack of continuity remained among the long time-series light data (Baugh et al., 2010). Therefore, continuity correction was required.

In cases where multiple sensors collected data for the same year, we calculated the average of the images as the NTL data for the year in question (Eq. (2)) (Elvidge et al., 2009).

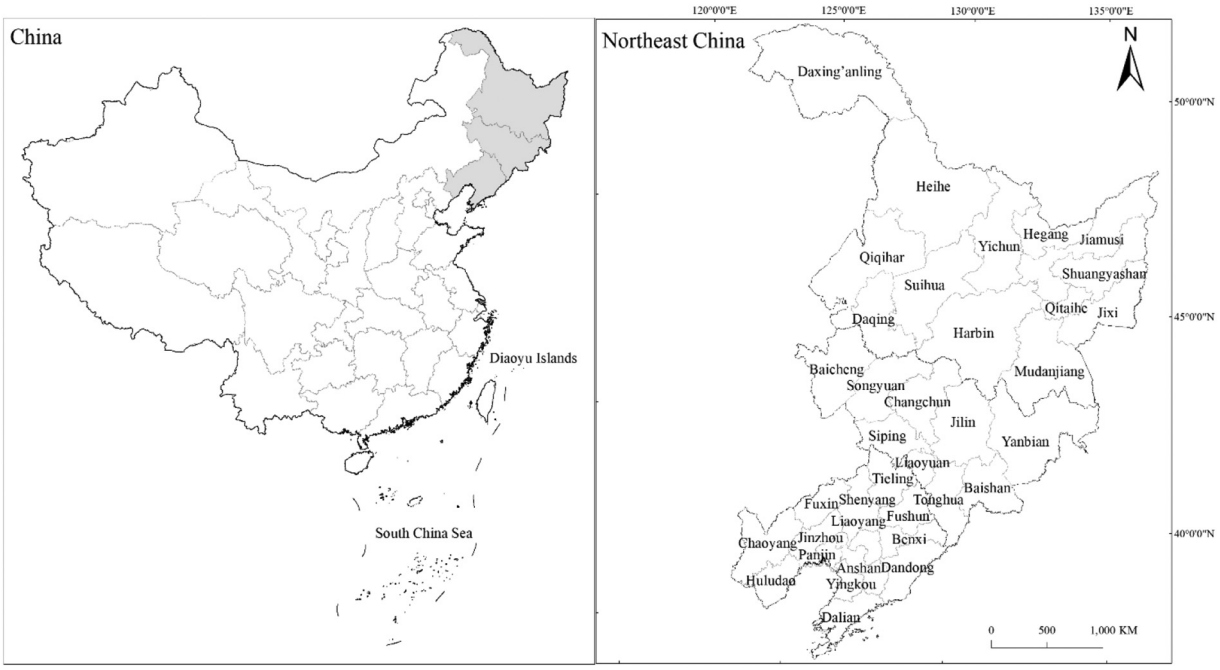

Fig. 1. Location of the study area.

$$DN_{(n,i)} = \begin{cases} 0 \; DN^{a}_{(n,i)} = 0 \; and \; DN^{b}_{(n,i)} = 0 \\ \left(DN^{a}_{(n,i)} + DN^{b}_{(n,i)}\right)/2 \; otherwise \end{cases} \quad (2)$$

Here, $DN^{a}_{(n,i)}$ indicates the light intensity of pixel i from sensor a in year n, while $DN^{b}_{(n,i)}$ stands for the light intensity of pixel i from sensor b in year n, and $DN_{(n,i)}$ is the corrected pixel value.

Previous studies have argued that the NTL intensity should always of the previous year should not be higher than that of the subsequent year for images of the same region (Cao et al., 2015; Liu et al., 2012a). Therefore, we intercalibrated images of different years using Eq. (3) (Cao et al., 2015).

$$DN_{(n,i)} = \begin{cases} 0 \; DN_{(n+1,i)} = 0 \\ DN_{(n-1,i)} \; DN_{(n+1,i)>0 \; and \; DN_{(n-1,i)>DN_{(n,i)}}} \\ DN_{(n,i)} \; others \end{cases} \quad (3)$$

Here, $DN_{(n-1,i)}$, $DN_{(n,i)}$, $DN_{(n+1,i)}$ are the light intensity values of the corrected pixels of three consecutive years after saturation and mean correction.

2.2.2. Processing of NPP images

Image reprojection, resampling, and cropping. To ensure minimal distortion of the image areas, we projected the images using the World Geodetic System 1984 (WGS84) and the Albers Equal Area Conic Coordinate System and resampled them with a 500-m spatial resolution. We then cropped the vector data based on the administrative boundaries of Northeast China to obtain the NPP-VIIRS NTL images of the region from 2012 and 2018.

Denoising. In NPP-VIIRS images, noise takes the form of negative and maximum values in the pixels, and there were pixels with negative values in the original NTL data. As a description of the metadata was lacking, these negative values were believed to be background noise created in the process of synthesizing data. Some studies substituted 0 for negative values (Zhou et al., 2015), and to ensure the integrity of the data and later calculations, we also adopted this practice. To remove the isolated excessively bright pixels, we arranged all the pixel values in an ascending order, denoted the pixel value at the 99th percentile as the DNM (decomposed Newton's method) threshold, and assigned the DNM value to all pixels higher than the threshold (Croft and A, 1978).

Selection of months. As population migration varies considerably by season (Qiao et al., 2013; Stathakis and Baltas, 2018) and light intensity can indirectly indicate population numbers, it was very important to select months with relatively little population migration. According to trends in the DN values of the NPP-VIIRS monthly light images between 2012 and 2018, we chose the light images of months with low levels of change to synthesize annual images for a given year, thus mitigating the impact of months with considerable migration due to holidays and other factors. We only downloaded data for March, April, September, November, and December for our selection, because data for May, June, and July were missing and many Chinese holidays occur in January, February, August, and October.

Table 1
Data source and description.

Date	Data	Resolution	Source	Details	Application
1992–2012	DMSP/OLS annual average NTL images	1000 m	NASA official website (https://www.ngdc.noaa.gov/eog/dmsp/downloadV4composites.html)	A total of 33 scenes, raster data	Population inversion
2012–2018	NPP-VIIRS moon composite NTL images	500 m	NASA official website (https://www.ngdc.noaa.gov/eog/viirs/download_dnb_composites.html)	A total of 60 scenes, raster data	Population inversion
2012–2018	Statistical population of permanent residents		National Bureau of Statistics website (http://www.stats.gov.cn/)	Statistical population of permanent residents, 2012–2018, Excel data	Calculation and verification
2017	Administrative Division data		National Census data (http://www.stats.gov.cn/)	Vector data	Research area display

NTL, nighttime light.

Table 2
DMSP image correction parameters.

Sensor number	Year	a	b	Sensor number	Year	a	b
F10	1992	0.60	1.32	F15	2000	0.81	1.18
	1993	0.71	1.30		2001	0.67	1.26
	1994	0.77	1.29		2002	0.59	1.28
F12	1994	0.65	1.31		2003	1.04	1.18
	1995	0.81	1.23		2004	1.15	1.08
	1996	1.03	1.14		2005	1.35	1.02
	1997	0.76	1.27		2006	1.25	1.07
	1998	0.69	1.24		2007	1.14	1.13
	1999	0.77	1.23	F16	2004	0.74	1.16
F14	1997	1.37	1.18		2005	0.90	1.18
	1998	0.97	1.22		2006	0.83	1.19
	1999	1.09	1.23		2007	0.73	1.21
	2000	0.10	1.18		2008	0.80	1.15
	2001	0.87	1.23		2009	0.61	1.15
	2002	0.99	1.18	F18	2010	0.34	1.21
	2003	0.90	1.20		2011	0.70	1.09
					2012	0.49	1.19

Image annualization and correction. We obtained the average of the suitable months within a given year to create annual images. Based on previous studies and the DMSP/OLS image processing, performed continuity correction on the annual NPP-VIIRS images (Eq. (4)) (Cao et al., 2015; Fan et al., 2013).

$$DN_{(n,i)} = \begin{cases} 0\ DN_{(n-1,i)} = DN_{(n,i)} = 0 \\ DN_{(n-1,i)}\ DN_{(n-1,i)} \geq DN_{(n,i)} \\ DN(n,i)\ DN_{(n,i)} > DN_{(n-1,i)} \end{cases} (n = 2012, 2013, \ldots, 2018) \quad (4)$$

Here, $DN_{(n,i)}$ denotes the value for the ith pixel of the nth year, and $DN_{(n-1,i)}$ denotes the value of the ith pixel of the $(n-1)$th year.

Continuity correction. According to previous literature and the DMSP data processing, the light intensity of the previous year should not exceed that of the subsequent year; thus, we intercalibrated the light images using Eq. (3).

2.2.3. Intercalibration of DMSP and NPP images

Due to the significant difference in spatial resolutions and radiation scales of the images obtained by the DMSP and NPP satellites, intercalibration was required to make the two sets of images comparable. As the datasets overlap in 2012, we analyzed the images of that year. Previous studies have shown a fairly robust relationship between DMSP and NPP data that follows the power function (Eq. (5)) (Li et al., 2017b; Zhao et al., 2019).

$$y = c \times x^d \quad (5)$$

Here, x refers to the DMSP/OLS value, and y refers to the NPP-VIIRS value; c and d are parameters. Therefore, based on Eq. (5), we corrected the 1992–2012 DMSP/OLS images.

2.2.4. Spatial modelling of population

Spatial analysis of population using NPP-VIIRS data. Previous literature published by domestic and international scholars demonstrates that NPP-VIIR NTL data are suitable for spatial population analyses (Li et al., 2017a; Shi et al., 2014; Wu et al., 2018). The relationship between population and NPP-VIIRS day/night band (DNB) NTL radiance satisfies the following formula (Eq. (6)):

$$\overline{POP} = ax^3 + bx^2 + cx + d \quad (6)$$

Here, $\overline{POP}$ is the result of the regression of municipal permanent residents and x is the radiance value for the NPP-VIIRS DNB. a, b, c, and d are the cubic polynomial coefficients. We assessed the precision of this relationship by calculating the relative error between the regression results and statistics as follows:

$$\gamma = \frac{|\overline{POP} - POP|}{POP} * 100\% \quad (7)$$

Here, γ is the relative error; POP is the regression outcome for the permanent municipal population, and POP is the permanent municipal population recorded in statistical data.

As we obtained a large relative error, it was necessary to process the data (Elvidge et al., 1997). Using the power function, we created correction factors for each year and each city to correct the NPP-VIIRS data, such that the population estimates for each city in each year would basically align with the actual statistics (Eq. (8)).

$$\begin{cases} c_n = POP_n / POP_{total} \\ f_n = c_n * DNB_n \end{cases} \quad (8)$$

Here, c is the correction factor, n is the year, POP_n is the statistical population of permanent residents in year n, POP_{total} is the statistical total population of permanent residents from 1992 to 2018, f is the adjusted light intensity, and DNB is the pre-adjusted light intensity.

Spatialization of population using DMSP/OLS data. Due to the lack of data from 1992 to 2011, we estimated the population based on the regression for the year 2012, while the 2012 population was estimated using the population spatialization method for DMSP/OLS data as outlined above.

3. Results

3.1. Spatial differentiation of population

The spatial distribution of population in Northeast China followed a T-shaped spatial clustering pattern with multiple centers, which were mainly provincial capitals (Fig. 2). The population tended to decrease toward the margins. Overall, Liaoning was more populated than Heilongjiang, which in turn was more populated than Jilin. From 2012, the regional population exhibited a trend of extreme negative growth. Within the six subsequent years, the region lost up to 4.46×10^6 residents. Among the three provinces, population loss was relatively more evident in Liaoning, which lost 7.42×10^6 residents between 1992 and 2018.

As shown in Figs. 3 and 4, and Table 3, before 2012, 13 cities saw an evident decline in population: Benxi, Chaoyang, Fushun, Huludao, Liaoyang, Panjin, Tieling, Yinkou, Baishan, Siping, Songyuan, Jiamusi, and Daqing. Meanwhile, the population rose in the other 23 cities. During this period, cities experiencing population loss were mainly small- or medium-sized, and the total population loss of the 13 cities amounted to 1.11×10^7 residents. After 2012, only Shenyang and Panjin experienced an increase in population. Growth skyrocketed in Shenyang—in 2018, its population was 7.45×10^6 people, an increase of 2.10×10^5 over that in 2012. In Panjin, the population increased by 1.00×10^4 from 2012 to 2018. However, the other 34 cities suffered population loss, losing a total of 4.67×10^6 residents.

3.2. Population loss in context

From 1992 to 1996, the populations in Northeast China displayed a positive linear growth trend, with the number of people growing by 5.64×10^4 over the four-year period at an average rate of 2.96×10^4. The population of the Liaoning province decreased during this period, with a loss of 2.96×10^4 people in four years, while those of Heilongjiang and Jilin grew; Jilin's population grew relatively slowly, increasing by 3.31×10^4, while Heilongjiang's population showed more obvious growth, increasing by 5.30×10^4.

From 1996 to 2006, the growth rate gradually slowed, with the total population of the three provinces decreasing by 1.11×10^7 people and the newly added population increasing by only 2.08×10^4, suggesting an average growth rate of only 0.18%. Given its large population, China

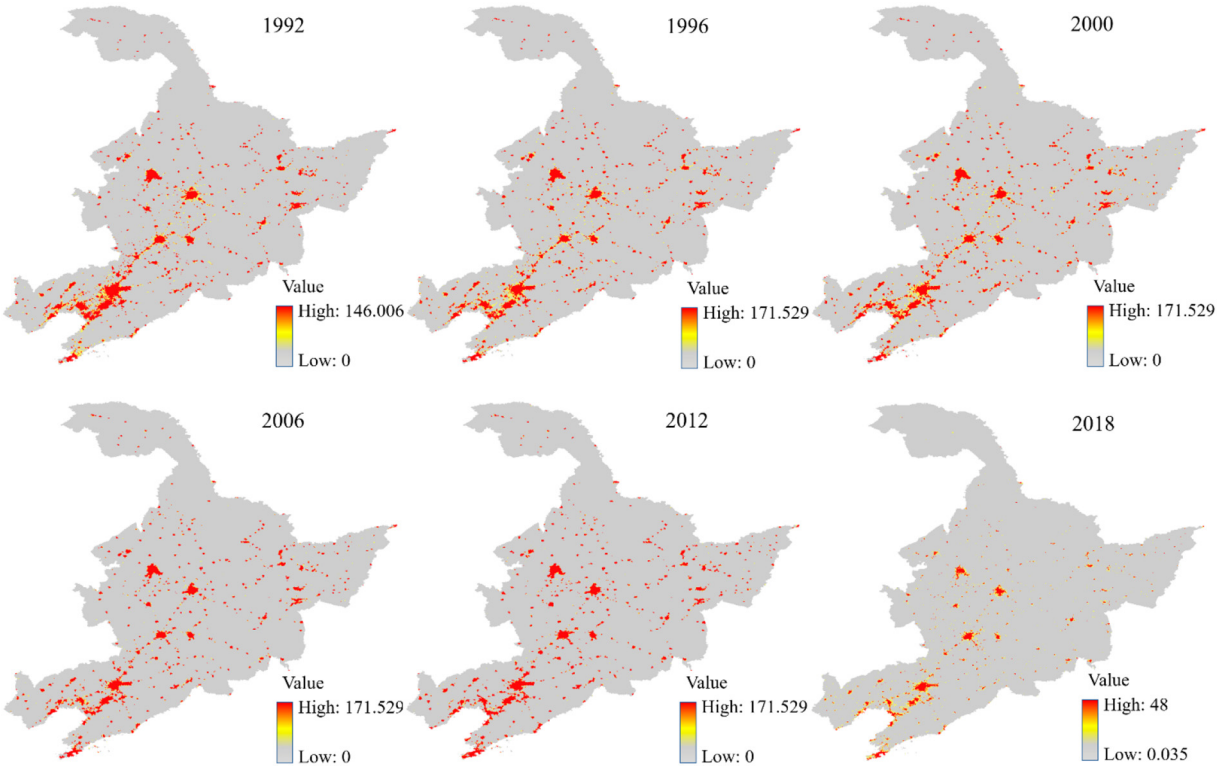

Fig. 2. Night light map of Northeast China.

implemented a family planning policy in 1982, and the effect of this policy is highly evident in Northeast China, where population growth was strongly controlled (Duan et al., 2013).

From 2006 to 2011, the population began to display a negative growth trend, with a population loss of 0.98×10^4 over the 5-year period and a decrease rate of 0.31%. To cope with population loss and an aging population, China has relaxed its second-child policy since the Third Plenary Session of the 18th CPC Central Committee in 2013 (Liu and Feng, 2014; Hou and Li, 2017). Since then, however, Northeast China has still experienced cliff-like population decline, particularly among those aged 15–65 (according to statistical data)(Qi et al., 2017), resulting in a critical loss of young adult labor and talent. Since 2012, steep population loss has continued in Northeast China, with all three provinces experiencing population outflow as high as 4.46×10^6 between 2012 and 2018.

4. Discussion

4.1. Impact of population loss

Population loss in Northeast China could affect labor supply, consumption, investment, and innovation, among other areas, which heavily undermines sustainable regional economic development, goes against the United Nations Sustainable Development Goals, and worsens inequalities both within China and between China and other nations.

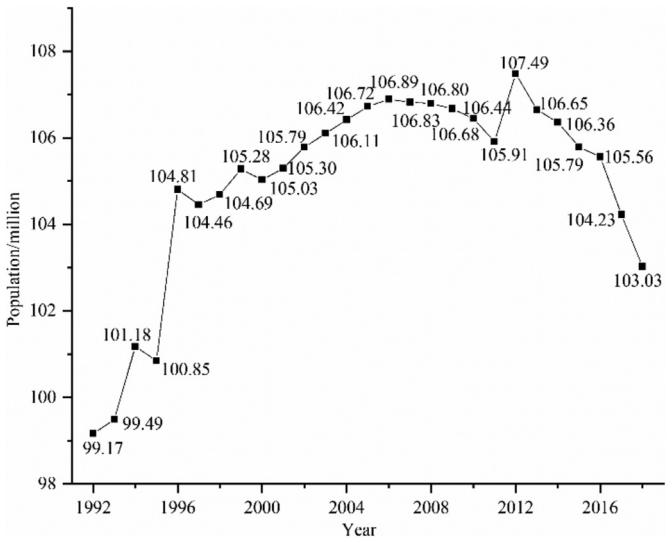

Fig. 3. Estimated total population of Northeast China, 1992–2018.

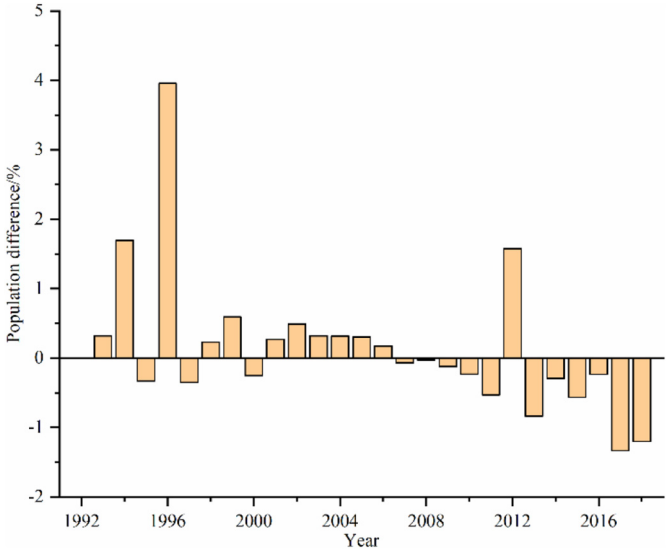

Fig. 4. Population growth rate of Northeast China, 1992–2018.

Table 3
Estimated population in Northeast China/million.

City	1992	1994	2000	2006	2012	2018	City	1992	1994	2000	2006	2012	2018
Shenyang	714.06	716.17	720.94	722.70	724.48	744.69	Tonghua	156.37	210.38	226.41	226.94	224.63	216.13
Dalian	559.83	569.23	580.26	585.97	589.71	504.96	Baishan	135.64	135.04	133.42	131.13	128.02	119.74
Anshan	283.02	306.51	341.43	347.80	350.28	342.16	Songyuan	313.12	309.36	306.18	299.14	289.82	275.11
Fushun	229.40	224.08	221.06	220.38	219.91	210.51	Baicheng	129.42	159.52	175.92	190.65	200.34	191.47
Benxi	378.29	302.20	192.36	173.52	152.84	146.50	Yanbian	64.07	114.14	164.41	190.63	213.08	209.22
Dandong	198.15	211.90	228.83	236.35	240.53	234.36	Harbin	559.14	620.69	907.41	985.11	999.12	954.40
Jinzhou	288.80	296.22	306.39	307.39	307.75	294.73	Qiqihar	475.48	504.19	523.01	539.14	559.07	529.91
Yingkou	372.56	337.54	269.93	252.76	235.20	231.37	Jixi	119.06	189.17	194.32	197.50	185.83	174.41
Fuxin	103.42	146.83	177.47	186.62	191.59	185.38	Hegang	98.77	73.45	119.09	104.24	108.24	99.76
Liaoyang	270.02	245.73	198.69	185.12	180.59	175.52	Shuangyashan	44.85	49.51	114.43	150.71	143.67	142.84
Panjin	136.85	134.39	130.28	129.76	128.82	129.85	Daqing	342.77	310.88	295.63	285.59	281.92	278.64
Tieling	413.55	387.43	316.24	306.51	302.02	292.04	Yichun	117.34	107.57	112.23	123.48	124.21	116.72
Chaoyang	507.03	459.34	423.54	360.31	340.70	335.35	Jiamusi	302.58	252.91	229.50	241.24	249.05	235.52
Huludao	391.03	331.07	295.29	287.39	279.98	276.12	Qitaihe	89.52	90.48	91.45	91.99	92.28	77.70
Changchun	733.59	741.21	753.20	756.01	757.27	751.77	Mudanjiang	84.12	153.82	192.55	219.87	258.87	249.82
Jilin	131.88	249.57	374.84	402.50	431.49	415.26	Heihe	91.84	114.28	135.25	152.44	172.73	159.55
Siping	459.95	426.69	374.04	361.17	335.99	318.81	Suihua	529.56	521.46	532.26	577.45	576.38	522.03
Liaoyuan	41.51	64.69	94.31	109.39	121.76	117.24	Daxing'anling	50.27	50.34	50.45	50.51	50.57	43.00

These negative impacts could manifest as low birth rates, a loss of talent and labor force, and intensified population aging (Chan et al., 2019; Carr, 2009; Zhang and Wu, 2017).

In recent years, population loss has continued to accelerate in Northeast China. In 2013, there was a "turning point" in population growth, meaning that growth shifted from positive to negative. The number of permanent residents in Northeast China dropped from 1.08×10^8 in 2012 to 1.07×10^8 in 2013 (Qi et al., 2017; Wang et al., 2011). Further, the natural growth rate of the population in the region was also lower than the national average, and even in this area, the region experienced negative growth.

Such population loss can lead to changes in the population structure, including increased population aging, which intensifies burdens regarding elder care and financial support. Between 2010 and 2015, the regional working population aged between 15 and 65 dropped from 8.67×10^7 to 8.50×10^7. Meanwhile, the proportion of the population aged 0–14, 15–64, and over 65 also changed by −0.81%, −1.73%, and 2.54%, respectively (Qi et al., 2017). In the context of profound transformation in socioeconomic development, the working population has migrated to economically advanced regions.

Finally, population loss can pose challenges for government policymakers and managers. Apparently random population movements in terms of residence and employment can lead to considerable shocks to social governance (Lankov et al., 2020; Li, 2020). In rural areas, huge population losses have given rise to the "empty nest" phenomenon, while urban population loss has resulted in shrinking cities (Duan et al., 2013; Liu and Cao, 2012). For instance, in Daxing'anling, the population was 5.00×10^5 before 2014, and the city was considered medium-sized. After 2014, when the population declined to below 4.80×10^5, Daxing'anling was ranked as a Type I small city.

4.2. Reasons for population loss in Northeast China

First, Northeast China has a simple economic and industrial structure with an underdeveloped private sector. As China's former industrial base, Northeast China made great contributions to the national economy before China's Reform and Opening Up; however, the region is now characterized by an over-concentration of heavy industries, such as kerosene production, automobile manufacturing, and aerospace technologies. Currently, confronted with many practical issues, such as insufficient production capacity, outdated technology, weak markets, and fierce competition, Northeast China is experiencing sluggish economic development. Talented individuals in this region cannot fully leverage their strengths, and thus have left the region in large numbers (Chen, 2005; Li et al., 2003; Liu and Li, 2009).

Second, with few large cities, Northeast China has yet to develop an influential metropolitan cluster. Only Harbin, Changchun, Shenyang, and Dalian can be regarded as large cities in the Chinese context, and except for Shenyang in Liaoning province, the provincial capitals are the only large cities. Further, Northeast China also cannot offer sufficient public resources to support in-migration by people from other provinces. As a result, in-migration has been concentrated in the urban conglomerates of the Yangtze River Delta and the Pearl River Delta. As Northeast China's large cities have scattered, it is challenging to form economically powerful urban circles (Ye et al., 2008; Yuan and Tang, 2006).

Third, limited development opportunities have also exacerbated population outflow. After the Reform and Opening Up, Southern China rapidly developed its economy and now has a more mature market economy, making it more attractive to talented individuals. South China not only surpasses Northeast China in many aspects, including housing options, business environment, education, and government functions, but also provides more development opportunities and relatively higher salaries, which have also contributed to population overflow in Northeast China (Duan et al., 2008; Li and Zhou, 2009).

4.3. Advantages of the research methodology

Traditional assessments of population loss mainly rely on statistical yearbooks (Liu and Feng, 2014; Qi et al., 2017). For example, from 2012 to 2018, yearbooks state that the city of Jiamusi in Heilongjiang province lost 6.12×10^4 people, but due to strong population mobility, statistical yearbook data can have errors and other issues. Based on our integration of NTL data with statistical data, we found that only 1.35×10^5 people were actually lost between 2012 and 2018, indicating a relative error of 121.16% in the statistical data. Based on this, we reconstructed the population data of 36 cities in Northeast China and found that the overall population loss was 4.46×10^8 during 2012–2018. Liaoning was the most populous province, followed by Heilongjiang and Jilin. Compared with the yearbook data, we determined that the overall population turnover in 2012–2018 was 9.83×10^4 fewer people, with population loss in 2013, 2017, and 2018, increasing by 3.761×10^5, 9.76×10^4, and 8.36×10^4, respectively, compared with that in 2012, 2016, and 2017.

4.4. Limitations

In this study, remote-sensing NTL images were employed to estimate population change, and the population data in the Statistical Yearbooks of China were used to build the model. Owing to the relatively

large errors in the statistical data themselves, issues with the satellite collecting the data, and noise during image shooting, the results of the study have a degree of errors and cannot be understood to represent the frequent residents in Northeast China with complete accuracy. Further, the statistics of some years were not complete during the time series used, and there were some errors in the model results. In future studies, we will leverage other models and algorithms to narrow the error as much as possible.

5. Conclusion

Using remote-sensing NTL images as a data source, we obtained the historical population data for the three provinces of Northeast China. Based on the prefecture-level population data extracted from the DN values of NTL images, we analyzed the spatial evolution of population between 1992 and 2018 and found that the region experienced different trends throughout the study period.

(1) The three northeastern provinces have great population mobility, presenting a multi-center "T"-shaped spatial pattern with provincial capitals being the main center and population gradually decreasing toward peripheral areas, with Liaoning > Heilongjiang > Jilin in terms of overall population.
(2) From 1992 to 1996, the population of the three northeastern provinces showed a positive linear growth trend, with the population increasing by 5.64×10^4 people and an average population growth rate of 2.29% over the four-year period; from 1996 to 2006, population growth slowed, with an increase of only 2.08×10^4 people over 10 years, and the average growth rate dropped to 0.18%; in 2006–2011, population growth showed a negative trend, with a population loss of 0.98×10^4 people and a decline rate of 0.31%; beginning in 2012, population loss was very serious, presenting a sharp linear decline, and by 2018, the population loss was as high as 4.46×10^6 people;
(3) Population loss will result in a series of negative effects in the region, not only affecting the population growth structure but also changing the regional population structure, and inconveniencing government management and planning.

CRediT authorship contribution statement

Haolin You: Data curation, Software, Writing – review & editing. **Jun Yang:** Conceptualization, Methodology, Software. **Bing Xue:** Data curation, Writing – review & editing. **Xiangming Xiao:** Writing – review & editing. **Jianhong Xia:** Visualization, Investigation, Writing – original draft. **Cui Jin:** Data curation, Writing – review & editing. **Xueming Li:** Writing – review & editing.

Declaration of competing interest

This manuscript has not been published or presented elsewhere in part or in entirety and is not under consideration by another journal. We have read and understood your journal's policies, and we believe that neither the manuscript nor the study violates any of these. There are no conflicts of interest to declare.

Acknowledgments

This study was supported by the National Natural Science Foundation of China (grant nos. 41771178, 42030409, 41630749), Liaoning Province Innovative Talents Support Program (grant no. LR2017017), and the Liaoning Province Outstanding Youth Program (grant no. LJQ2015058). The authors would like to acknowledge the contributions of all the experts in building the model and formulating the strategies in this study. This work was supported by National Key R&D Program of China (Re: 2017YFC0506403).

References

Adams, R.H., Page, J., 2005. Do international migration and remittances reduce poverty in developing countries? World Dev. 33 (10), 1645–1669.
Baugh, K., Elvidge, C.D., Ghosh, T., Ziskin, D., 2010. Development of a 2009 stable lights product using DMSP-OLS data. Proceedings of the Asia-Pacific Advanced Network 30.
Cao, Z., Wu, Z., Kuang, Y., Huang, N., 2015. Correction of DMSP/OLS night-time light images and its application in China. J. Geo-Information Sci. 17 (09), 1092–1102.
Carr, D., 2009. Population and deforestation: why rural migration matters. Prog. Hum. Geogr. 33 (3), 355–378.
Chan, E.K.F., Timmermann, A., Baldi, B.F., Moore, A.E., Lyons, R.J., Lee, S., Kalsbeek, A.M.F., Petersen, D.C., Rautenbach, H., Förtsch, H.E.A., Bornman, M.S.R., Hayes, V.M., 2019. Human origins in a southern African palaeo-wetland and first migrations. Nature 575 (7781), 185–189.
Chen, L., 2005. Availing foreign-investment strategies of industrial structure development in the northeast industrial base. Econ. Geogr. 05, 624–628.
Croft, A, T., 1978. Nighttime images of the earth from space. Sci. Am. 239 (1), 86–98.
Duan, C., Yang, G., Zhang, F., Lu, X., 2008. Nine trends in China's floating population since the reform and opening up. Popul. Res. 06, 30–43.
Duan, C., Lv, L., Zou, X., 2013. Major challenges for China's floating population and policy suggestions: an analysis of the 2010 population census data. Popul. Res. 37 (2), 17–24.
Elvidge, C.D., Baugh, K.E., Kihn, E.A., Kroehl, H.W., Davis, E.R., Davis, C.W., 1997. Relation between satellite observed visible-near infrared emissions, population, economic activity and electric power consumption. Int. J. Remote Sens. 18 (6), 1373–1379.
Elvidge, C.D., Ziskin, D., Baugh, K.E., Tuttle, B.T., Ghosh, T., Pack, D.W., Erwin, E.H., Zhizhin, M., 2009. A fifteen year record of global natural gas flaring derived from satellite data. Energies 2 (595–622).
Fan, C.C., 2005. Interprovincial migration, population redistribution, and regional development in China: 1990 and 2000 census comparisons. Prof. Geogr. 57 (2), 295–311.
Fan, J., Ma, T., Zhou, C., Zhou, Y., 2013. Changes in spatial patterns of urban landscape in Bohai Rim from 1992 to 2010 using DMSP-OLS data. J. Geo-Information Sci. (2), 126–134.
Ferracioli, L. (2018). International Migration and Human Rights. United Nations, 16(1), 197–210.
Fu, Q., Posth, C., Hajdinjak, M., Petr, M., Mallick, S., Fernandes, D., Furtwängler, A., Haak, W., Meyer, M., Mittnik, A., Nickel, B., Peltzer, A., Rohland, N., Slon, V., Talamo, S., Lazaridis, I., Lipson, M., Mathieson, I., Schiffels, S., Skoglund, P., Derevianko, A.P., Drozdov, N., Slavinsky, V., Tsybankov, A., Cremonesi, R.G., Mallegni, F., Gély, B., Vacca, E., Morales, M.R.G., Straus, L.G., Neugebauer-Maresch, C., Teschler-Nicola, M., Constantin, S., Moldovan, O.T., Benazzi, S., Peresani, M., Coppola, D., Lari, M., Ricci, S., Ronchitelli, A., Valentin, F., Thevenet, C., Wehrberger, K., Grigorescu, D., Rougier, H., Crevecoeur, I., Flas, D., Semal, P., Mannino, M.A., Cupillard, C., Bocherens, H., Conard, N.J., Harvati, K., Moiseyev, V., Drucker, D.G., Svoboda, J., Richards, M.P., Caramelli, D., Pinhasi, R., Kelso, J., Patterson, N., Krause, J., Pääbo, S., Reich, D., 2016. The genetic history of Ice Age Europe. Nature 534 (7606), 200–205.
Fukuda-Parr, Sakiko, 2016. From the millennium development goals to the sustainable development goals: shifts in purpose, concept, and politics of global goal setting for development. Gend. Dev. 1–10.
Guo, A., Yang, J., Sun, W., Xiao, X., Xia Cecilia, J., Jin, C., Li, X., 2020. Impact of urban morphology and landscape characteristics on spatiotemporal heterogeneity of land surface temperature. Sustain. Cities Soc. 63, 102443.
He, B.J., 2018. Potentials of meteorological characteristics and synoptic conditions to mitigate urban heat island effects. Urban Clim. 24, 26–33.
Bao-Jie, He, Lan, Ding, Deo, & Prasad. (2019). Enhancing urban ventilation performance through the development of precinct ventilation zones: A case study based on the greater Sydney, Australia - ScienceDirect. Sustain. Cities Soc., 47(C), 101472.
Hou, J., Li, X., 2017. The analysis of the status of China's floating elderly population and It's influencing factors. Popul. J. 6.
Lankov, A., Ward, P., Kim, J., 2020. The north Korean Workers in Russia: problematizing the "forced labor" discourse. Asian Perspect. 44 (1), 31–53.
Li, D., 2020. Islands of sovereignty: Haitian migration and the borders of empire by Jeffrey S. Kahn (review). Anthropol. Q. 93 (1), 1659–1663.
Li, F., Zhou, C., 2009. Spatial autocorrelation analysis on regional economic disparity of northeast economic region in China. Chin. J. Pop. Resour. Environ. 7 (2), 27–31.
Li, G., Li, P., Tan, X., Liu, X., 2003. Situation and countermeasures of industrial structure adjustment and escalation of Northeast China. Sci. Geogr. Sin. 01, 7–12.
Li, X., Chen, Z., Wu, J., Wang, W., Qu, L., Zhou, C., Han, X., 2017a. Gridding methods of city permanent population based on night light data and spatial regression models. J. Geo-info. Sci. 19 (10), 1298–1305.
Li, X., Li, D., Xu, H., Wu, C., 2017b. Intercalibration between DMSP/OLS and VIIRS nighttime light images to evaluate city light dynamics of Syria 's major human settlement during Syrian Civil War. Int. J. Remote Sens. 38 (21), 5934–5951.
Liu, T., Cao, G.Z., 2012. Agglomeration and dispersion of city sizes and the influence of central cities:based on the multi-scale spatial autocorrelation and the case of China. Geogr. Res. 31 (7), 1317–1327.
Liu, Y., Feng, J., 2014. Characteristics and impact factors of migration in China: based on the analysis of the sixth census data. Hum. Geogr. 29 (02), 129–137.
Liu, Y., Li, G., 2009. Regulation model and mechanism of urbanization response to the industrial structure evolvement in Northeast China. Acta Geograph. Sin. 064 (002), 153–166.
Liu, Z., He, C., Zhang, Q., Huang, Q., Yang, Y., 2012a. Extracting the dynamics of urban expansion in China using DMSP-OLS nighttime light data from 1992 to 2008. Landsc. Urban Plan. 106 (1), 62–72.
Liu, W., Wang, L., Chen, Z., 2012b. Flow field and its regional differentiation of interprovincial migration in China. Econ. Geogr. (02), 8–13.

Liu, R., Li, T., Greene, R., 2020. Migration and inequality in rental housing: affordability stress in the Chinese cities. Appl. Geogr. 115, 102138.
Lutz, W., Neill, B.C.O., Scherbov, S., 2003. Europe's Population at a Turning Point (SCIENCE).
Mei, G., Dong, L., Tian, C., Lina, K.E., 2014. The research for Liaoning environmental efficiency and spatial-temporal differentiation. Geogr. Res. 33 (12), 2345–2357.
Mitsuru, K., 2018. Economic consequences of population aging in Japan: effects through changes in demand structure. Singap. Econ. Rev. 110, S814729885.
Nash, K.L., Blythe, J.L., Cvitanovic, C., Fulton, E.A., Blanchard, J.L., 2020. To achieve a sustainable blue future, progress assessments must include interdependencies between the sustainable development goals. One Earth.
Nijman, J., Wei, Y.D., 2020. Urban inequalities in the 21st century economy. Appl. Geogr. 117, 102188.
Oke, T.R., 1973. City size and the urban Heat Island. Atmos. Environ. (1967) 7 (8), 769–779.
Otterstrom, S.M., 2001. Trends in national and regional population concentration in the United States from 1790 to 1990: from the frontier to the urban transformation. Soc. Sci. J. 38 (3), 393–407.
Qi, W., Liu, S., Jin, F., 2017. Calculation and spatial evolution of population loss in Northeast China. Sci. Geogr. Sin. 37 (12), 1795–1804.
Qiao, Z., Tian, G., Xiao, L., 2013. Diurnal and seasonal impacts of urbanization on the urban thermal environment: A case study of Beijing using MODIS data. ISPRS J. Photogramm. Remote Sens. 85 (nov.), 93–101.
Qiao, Z., Liu, L., Qin, Y., Xu, X., Liu, Z., 2020. The impact of urban renewal on land surface temperature changes: a case study in the Main City of Guangzhou, China. Remote Sens. 12 (5), 794.
Shi, K., Yu, B., Huang, Y., Hu, Y., Yin, B., Chen, Z., Chen, L., Wu, J., 2014. Evaluating the ability of NPP-VIIRS nighttime light data to estimate the gross domestic product and the electric power consumption of China at multiple scales: a comparison with DMSP-OLS data. Remote Sens. 6 (2), 1705–1724.
Simini, F., González, M.C., Maritan, A., Barabási, A., 2012. A universal model for mobility and migration patterns. Nature 484 (7392), 96–100.
Stathakis, D., Baltas, P., 2018. Seasonal population estimates based on night-time lights. Comput. Environ. Urban. Syst. 68, 133–141.
Stewart, I.D., Oke, T.R., 2012. Local climate zones for urban temperature studies. Bull. Am. Meteorol. Soc. 93 (12), 1879–1900.
Sun, P., Ding, S., Xiu, C., Wei, Y., 2012. Population-economy-space urbanization of Northeast China. Sci. Geogr. Sin. 32 (4), 450–457.
Wang, S.J., Yang, S., Feng, Z.X., Jiang, L.L., 2011. Pattern and Progress of large urban agglomerations and urban flows intensity in Northeast China. Sci. Geogr. Sin. 31 (3), 287–294.
Wang, G., Pan, Z., Lu, Y., 2012. China's inter-provincial migration patterns and influential factors: evidence from year 2000 and 2010 population census of China. Chin. J. Popul. Sci. (05), 4–15.
Wu, R., Yang, D., Dong, J., Zhang, L., Xia, F., 2018. Regional inequality in China based on NPP-VIIRS night-time light imagery. Remote Sens. 10 (2), 240.
Yang, X., And, Y.H., Chen, B., 2011. Observed surface warming induced by urbanization in east China. J. Geophys. Res.-Atmos. 116 (D14). https://doi.org/10.1029/2010jd015452.
Yang, X., Yue, W., Gao, D., 2013. Spatial improvement of human population distribution based on multi-sensor remote-sensing data: an input for exposure assessment. Int. J. Remote Sens. 34 (15–16), 5569–5583.
Yang, J., Wang, Y., Xiu, C., Xiao, X., Xia, J., Jin, C., 2020a. Optimizing local climate zones to mitigate urban heat island effect in human settlements. J. Clean. Prod. 275, 123767.
Yang, J., Zhan, Y., Xiao, X., Xia, J.C., Sun, W., Li, X., 2020b. Investigating the diversity of land surface temperature characteristics in different scale cities based on local climate zones. Urban Clim. 34, 100700.
Ye, Y., Li, Y., Ni, K., 2008. The migration within Beijing-Tianjin-Hebei Metropolitan Area and integrated development in urban and rural areas. Chin. J. Popul. Sci. 2 57–64+96.
You, H., Jin, C., Sun, W., 2020. Spatiotemporal evolution of population in Northeast China during 2012–2017: a nighttime light approach. Complexity 2020, 1–12.
Yu, T., Song, Y., Hao, F., A, R., 2017. Space pattern evolution of population distribution and the driving factors in Northeast China. Sci. Geogr. Sin. 37 (05), 709–717.
Yuan, X., Tang, X., 2006. Megalopolitanization: A new strategy of urbanization in China. China Popul. Resourc. Environ. (4), 7–12.
Yue, W., Liu, X., Zhou, Y., Liu, Y., 2019. Impacts of urban configuration on urban heat island: an empirical study in China mega-cities. Sci. Total Environ. 671, 1036–1046.
Zhang, J., Wu, L., 2017. Influence of human population movements on urban climate of Beijing during the Chinese New Year holiday. Sci. Rep. 7 (1).
Zhang, M., He, Z., Fan, Y., 2017. Calibration for DMSP/OLS stable nighttime light images. Bull. Surv. Map. 489 (12), 63–67.
Zhao, M., Zhou, Y., Li, X., Zhou, C., Cheng, W., Li, M., & Huang, K. (2019). Building a series of consistent night-time light data (1992–2018) in Southeast Asia by integrating DMSP-OLS and NPP-VIIRS. IEEE transactions on geoscience and remote sensing.
Zhou, Y., Ma, T., Zhou, C., Xu, T., 2015. Nighttime light derived assessment of regional inequality of socioeconomic development in China. Remote Sens. 7 (2), 1242–1262.
Zhu, S., Yu, C., He, C., 2020. Export structures, income inequality and urban-rural divide in China. Appl. Geogr. 115, 102150.